Journal of Materials Chemistry C

Accepted Manuscript

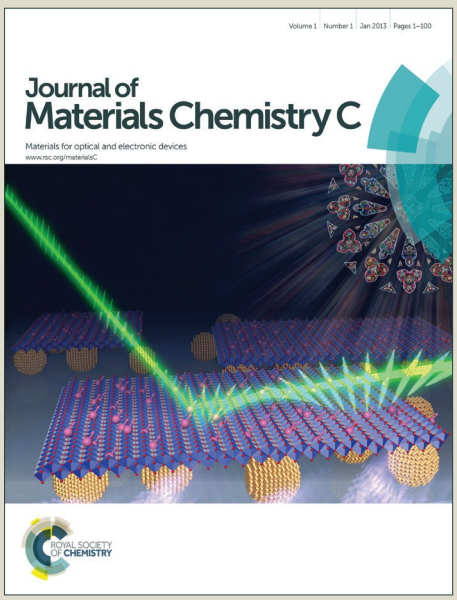

ROYAL SOCIETY OF CHEMISTRY

www.rsc.org/materialsC

Polyethylenimine-interlayered silver-shell magnetic-core microspheres as a multifunctional SERS substrate

Chongwen Wang‡[ab], Jiawen Xu‡[bc], Junfeng Wang[d], Zhen Rong[a], Ping Li[a], Rui Xiao[b*] and Shengqi Wang[ab*]

The fabrication of an ideal noble metal modified magnetic microsphere as high performance SERS substrate that possesses good dispersibility, strong magnetic responsiveness, and high sensitivity is still a challenge. Herein, we reported a novel route to fabricating Ag-coated magnetic core-shell microspheres (Fe_3O_4@PEI@Ag) with most of the desired advantages by using polyethyleneimine (PEI) as an interlayer. The size and coverage level of the Ag-NPs shell on Fe_3O_4@PEI@Ag microspheres were easily controlled by varying the amount of $AgNO_3$. Meanwhile, the magnetic core endowed the Fe_3O_4@PEI@Ag microspheres with superior magnetic nature, which enabled convenient separation and further enhanced Raman signals due to enrichment of targeted analytes and abundant interparticle hotspots created by magnetism-induced aggregation. Considering these features, the Fe_3O_4@PEI@Ag is expected to be a versatile SERS substrate, which was verified by the detection of adsorbed PATP molecules and human IgG with a detection limit as low as 10^{-11} M and 10^{-14} g/mL, respectively. Therefore, the novel Fe_3O_4@PEI@Ag microsphere has an enormous potential for practical SERS detection applications, especially in the target protein quantitative detection field.

INTRODUCTION

Surface-enhanced Raman scattering (SERS) is a powerful fingerprint vibrational spectroscopy with high sensitivity, and it is widely used in biochemical detection, analytical chemistry, environment monitoring and biological sensing.[1-3] All these applications are based on proper utilization of "free-electron-like" metal materials, such as Au, Ag, and Cu, and only these noble metal structures with rough surface can provide obvious SERS effect.[4] Therefore, the key of its prominent application lies in fabricating high performance SERS substrates. So far, researchers have fabricated many SERS substrates, among which metal film over periodic nanostructure and Au/Ag colloids in suspension are extensively utilized.[5] The periodic nanostructure can achieve well sensitivity and high reproducibility, but has disadvantages of high cost and difficult to be further chemically modified. Au/Ag colloidal nanoparticles are more efficient with flexible control over individual geometry, easy to mass fabricate, and have good biocompatibility.[6] However, the drawbacks of Au/Ag colloid substrates are their limited enhancement ability and poor stability.[7] Therefore, a reliable and practical SERS substrate with high sensitivity is still a challenge. It should be noted that, up to now, the main problem of SERS detection is that it is difficult to conduct quantitative analysis and hard to apply in the complex system only depend on the noble metal SERS substrate itself.

Magnetic microspheres have been extensively investigated for various applications.[8] Due to their excellent magnetic responsiveness, magnetic microspheres can assist in convenient recycling of novel metals, magnetic enrichment of analytes and rapid separation from reaction system.[9, 10] Recently, noble metal modified magnetic microspheres have attracted more attention, due to the combined functions of optical and magnetic properties from the two component materials, especially as active SERS substrates.[11, 12] These composite structures can be used to actively concentrate the target analyte in the sample solution, and then be conveniently immobilized on Si wafer under an external magnet. Among them, Ag-coated magnetic core-shell microspheres, which have the advantages of high SERS activity of Ag shell，good magnetic responsiveness of larger Fe_3O_4 core, and relatively facile fabrication process, is the most promising one. The most frequently used method of Ag-coated magnetic

microspheres synthesis is forming a certain thickness of silica or carbon shell first for stabilization of whole particle structures as well as providing sites for in situ reduction of local Ag^+ ions.[13-17] However, there are still two major stumbling blocks remaining to be overcome in these fabrication methods. Firstly, it is hard to obtain well-dispersed and uniform Ag coated magnetic composites, because magnetic attraction often brings in aggregation among particles during the Ag shell coating process. The irregular aggregation would affect both the structural homogeneity, and the reproducibility of SERS signals when used as SERS substrate. For example, although An et al. fabricated Fe_3O_4@C@Ag microspheres with different concentrations of $AgNO_3$, the ferromagnetic property of the magnetic cores made the final composite microspheres aggregate severely.[13] Secondly, the shell coating or growing process may greatly weaken the magnetic responsiveness of the Ag-modified magnetic composites, which would result in time consuming and sample wasting. For instance, Wang's group reported a general route to preparing magnetic-based silver composite microspheres with a 250 nm SiO_2 shell exhibiting well-dispersed performance, but the thick SiO_2 shell seriously affected the saturated magnetization of the product, which lengthened the detection time obviously.[15] Due to these obstacles, Fe_3O_4@Ag microspheres with both good dispersity and strong magnetic responsiveness have been scarcely reported. The absence of high quality Ag-coated magnetic composite microspheres seriously limit their widely application.

In this work, we reported a highly reproducible way to synthesize a novel polyethylenimine-interlayered silver-shell magnetic-core microspheres (Fe_3O_4@PEI@Ag). The cationic polyethyleneimine (PEI) is skillfully used to form a bifunctional thin shell, which not only prevents magnetic particles from aggregation, but also facilitates absorption dense 3 nm Au NPs as seeds to grow uniform Ag-NPs shells. To the best of our knowledge, this is the first report of using polymer PEI to prepare high-performance Fe_3O_4@Ag core-shell microspheres with good dispersity, strong magnetic responsiveness, and highly reproducible structure. The SERS activities of as-prepared Fe_3O_4@PEI@Ag microspheres have been tested by using PATP as probe molecule. Furthermore, these Fe_3O_4@PEI@Ag microspheres were successfully applied to SERS based immunoassay for human immunoglobulin (IgG) detection. Considering these features, the Fe_3O_4@PEI@Ag microspheres with excellent SERS ability, good signal reproducibility, and excellent speed of magnetic enrichment can be potentially used as an effective and versatile SERS substrate in practical applications, including environment monitoring, food safety, pollutant detection, etc. Especially, with the help of SERS-tag, the Fe_3O_4@PEI@Ag microspheres have the potential to do quantitative detection in the complex system.

METHODS

Materials and chemicals.

Silver nitrate, Ferric chloride ($Fe_3O_4.6H_2O$), Ethylene glycol, formaldehyde (37%), ammonia (28%) were purchased from Sinopharm Chemical Reagent Co. PATP, hexadecyltrimethylammonium bromide (CTAB), 11-mercaptoundecanoic acid (MUA), p-Aminothiophenol (PATP), 2-nitrobenzoic acid (DTNB), Polyethyleneimine branched (PEI, MW 25000), Polyvinylpyrolidone (PVP, MW 40000) were purchased from Sigma-Aldrich Chemicals Co. and all other chemicals were purchased from Shanghai Chemical Reagent Co., Ltd. Human IgG, goat anti human IgG and mouse anti human IgG were purchased from Beijing Biosynthesis Biotechnology Co., Ltd. Bovine serum albumin (BSA) was purchased from Invitrogen Biotechnology Co., Ltd. All reagents were of analytical grade and were used without further purification. All aqueous solutions were made with Millipore ultrapure water (purified with Milli-Q system, 18.2 MΩ cm^{-1}).

Instruments

Transmission electron microscope (TEM) images and high resolution TEM images were taken on a Hitachi H-7650 TEM and JEOL-2010 HRTEM at an accelerating voltage of 200 kV. Samples dispersed at a proper concentration were cast onto a carbon-coated copper grid. Scanning electron microscope (SEM) was performed

with a JEOL JSM-7001F microscopy at an accelerating voltage of 5 kV. Samples dispersed at an appropriate concentration were cast onto a Si wafer at room temperature and sputter-coated with Pt. Zeta potential measurements were conducted with a Nano ZS Zetasizer (model ZEN3600, Malvern Instruments) using a He-Ne laser at a wavelength of 632.8 nm. The crystalline structure was investigated by X-ray power diffraction (RIGAK, D/MAX 2550 VB/PC, Japan), and the magnetic properties of the resulting products were investigated using a superconducting quantum interference device magnetometer (SQUID, MPMSXL-7) at 300 K. UV-vis spectra were measured by a Shimadzu 2600 spectrometer. Samples were placed in quartz cells of 1 cm optical path, after dilution to 5% in Milli-Q water (v/v). Raman spectra was recorded on a portable Raman system (B&W Tek, i-Raman Plus BWS465-785H spectrometer) with 785 nm laser excitation. Its maximum laser power on the sample was 275 mW, which was measured using a power meter (Coherent, lasercheck). The back-illuminated CCD cooled at -2 °C was used as the detector. Five spectra from different sites of each sample were collected and averaged to represent the SERS result. The measured spectra were presented after adjusting the baselines for comparison.

Synthesis of Fe_3O_4 nanoparticles.

The magnetic particles (250 nm) were synthesized through a modified solvothermal reaction.[18] Typically, 2.7 g of $FeCl_3.6H_2O$ was dissolved in 80 mL of ethylene glycol under magnetic stirring for 30 min. Subsequently, 5.4 g of NaAc and 2 g of PEG6000 were added to this solution and stirred until the reactants were fully dissolved. Then, the mixture was transferred into a Teflon-lined autoclave (100 mL capacity) and heated at 210 °C for 6 h. The products were collected with the help of a magnet, followed by washing with deionized water and ethanol three times each. The final product was dried under vacuum at 60 °C for 6 h for future use.

Preparation of Fe_3O_4@PEI-Au seed nanoparticles

The Fe_3O_4@PEI nanoparticles were synthesized through a PEI self-assembly process under sonication condition. First, 0.25g PEI was dissolved in 50 mL of deionized water by ultrasonication for 10 min. Next, 0.2 g prepared Fe_3O_4 microspheres were dispersed in the PEI solution under sonication for 2 h, during which PEI gradually self-assembled on the Fe_3O_4 microspheres. Then Fe_3O_4@PEI microspheres were magnetically separated and rinsed five times with deionized water. Meanwhile, 3~5 nm Au nanoparticles were prepared according to the YouXing Fang' method.[19] Briefly, 200 mL of aqueous solution containing 0.25 mM $HAuCl_4$ and 0.25 mM trisodium citrate was prepared in a conical flask with vigorous stirring at room temperature. Then 6 mL of 0.1 mol/L freshly prepared $NaBH_4$ solution was added rapidly to the solution, which caused the solution to turn pink immediately, indicating the formation of Au NPs. Then, PEI-modified Fe_3O_4 nanoparticles were mixed with colloidal 3 nm Au NPs and sonicated for 1 h to form Fe_3O_4@PEI-Au seed. Finally, Fe_3O_4@PEI-Au seed were magnetically separated from excess Au colloid solution and rinsed three times with deionized water.

Preparation of monodispersed Fe_3O_4@PEI@Ag microspheres

10 mg Fe_3O_4@PEI-Au seed was dispersed in 100 mL 0.15 mM silver nitrate aqueous solution containing 0.2 wt% PVP, then the excessive amount of 37% formaldehyde (150 μL) and 25% ammonia solution (300 μL) were added in sequence. The Fe_3O_4@PEI@Ag core-shell microspheres were obtained within 2 min under sonication at 30 °C. The products were magnetically separated and rinsed five times with deionized water to remove the excess PVP.

Preparation of SERS tags (Au NRs-DTNB) for the SERS immunoassay

Au nanorods (Au NRs) were synthesized following the surfactant-assisted, seed-mediated method developed by Nikoobakht with some modifications.[20] First, the seed solution was first prepared by mixing 5 ml of 0.1M CTAB solution with 42 uL of 29 mM $HAuCl_4$, then 0.3 ml of 10 mM $NaBH_4$ were added with vigorous stirring for 10 min. Second, the resulting seed solution were used in prepare of Au nanorods. Briefly, 0.4 mL of 10 mM $AgNO_3$ was added to 40 mL of 0.1 M CTAB solution, then 0.8 ml of 29 mM $HAuCl_4$ were added and mixed. To this solution 0.32 mL of 0.1 M ascorbic acid was added with gentle mixing. Finally, 130 uL of seed solution were added and the entire solution was kept at 30 °C overnight without any further stirring.

DTNB molecules were used as Raman reporters for the SERS immunoassay.[21, 22] DTNB-functionalized Au NRs (Au NRs-DTNB) were prepared in accordance with the following procedure. First, 10 μL of freshly prepared DTNB ethanol solution (10 mM) was added into 10 mL of the as-prepared Au NRs solution, and the resultant mixture was vigorously stirred at 30 °C for 1 h under sonication. The resulting solution was centrifuged at 7000 rpm for 6 min to remove the excess DTNB molecules, and the precipitate was redispersed in 10 mL of deionized water.

Fe_3O_4@PEI@Ag based SERS immunoassay protocol

The immuno-Fe_3O_4@PEI@Ag microspheres and immune-Au NRs-DTNB were prepared by conjugating an amine of antibodies to carboxyl-coated nanostructures through the EDC/sulfo-NHS chemistry.[23] Fe_3O_4@PEI@Ag (10 mg/mL) were incubated overnight with vigorous sonication in an ethanolic solution containing 1 mM MUA. Then, EDC (100 μL, 10 mM) and sulfo-NHS (20 μL, 0.1 M) were added to 100 μL of the solution containing carboxyl group-functionalized Fe_3O_4@PEI@Ag. The mixture was shaken for 15 min, then 0.5 mL of 3 mg/mL goat anti-human IgG was added, and the mixture was shaken for 2 h. To block the unreacted carboxyl sites on the Fe_3O_4@PEI@Ag surface, 0.5 mL of 10 mg/mL BSA was added to the mixture and allowed to react for an additional 1 h. To remove any excess unbound antibody, the solution was centrifuged at 3000 rpm for five buffer exchanges (50 mM borate buffer, pH 8.3). Finally，the products were stored at 4 °C before use. The preparation of immune-Au NRs-DTNB is similar with mmuno-Fe_3O_4@PEI@Ag. After coupling with mouse anti-human IgG, the immune-Au NRs-DTNB solution was filtered through a 0.2 μm syringe filter to remove any aggregates. Then, the products were stored at 4 °C before use.

SERS measurements

PATP was used as the Raman probe for SERS measurements. The detail operation process was as illustrated in Scheme 1(b). A series of PATP alcoholic solutions were applied in the SERS examination of Fe_3O_4@PEI@Ag microspheres synthesized with different amounts of $AgNO_3$. Each tube of freshly prepared PATP solution (1 mL) was mixed with 2 μL of as-prepared microspheres dispersion (5 mg/mL), and the mixture was mildly sonicated for 30 min, therefore allowing adequate molecular adhesion. Afterwards, the Fe_3O_4@PEI@Ag microspheres were separated from the solution by a magnet, and then the precipitate was transferred onto a clean Si wafer, and analyzed with the Raman spectrometer. SERS signals were recorded. Power at samples was 20 % of the full laser power while integration time was 10 s. The operating principle of the Fe_3O_4@PEI@Ag based SERS immunoassay was performed similarly, as illustrated in Scheme 1(c).

RESULTS AND DISCUSSION

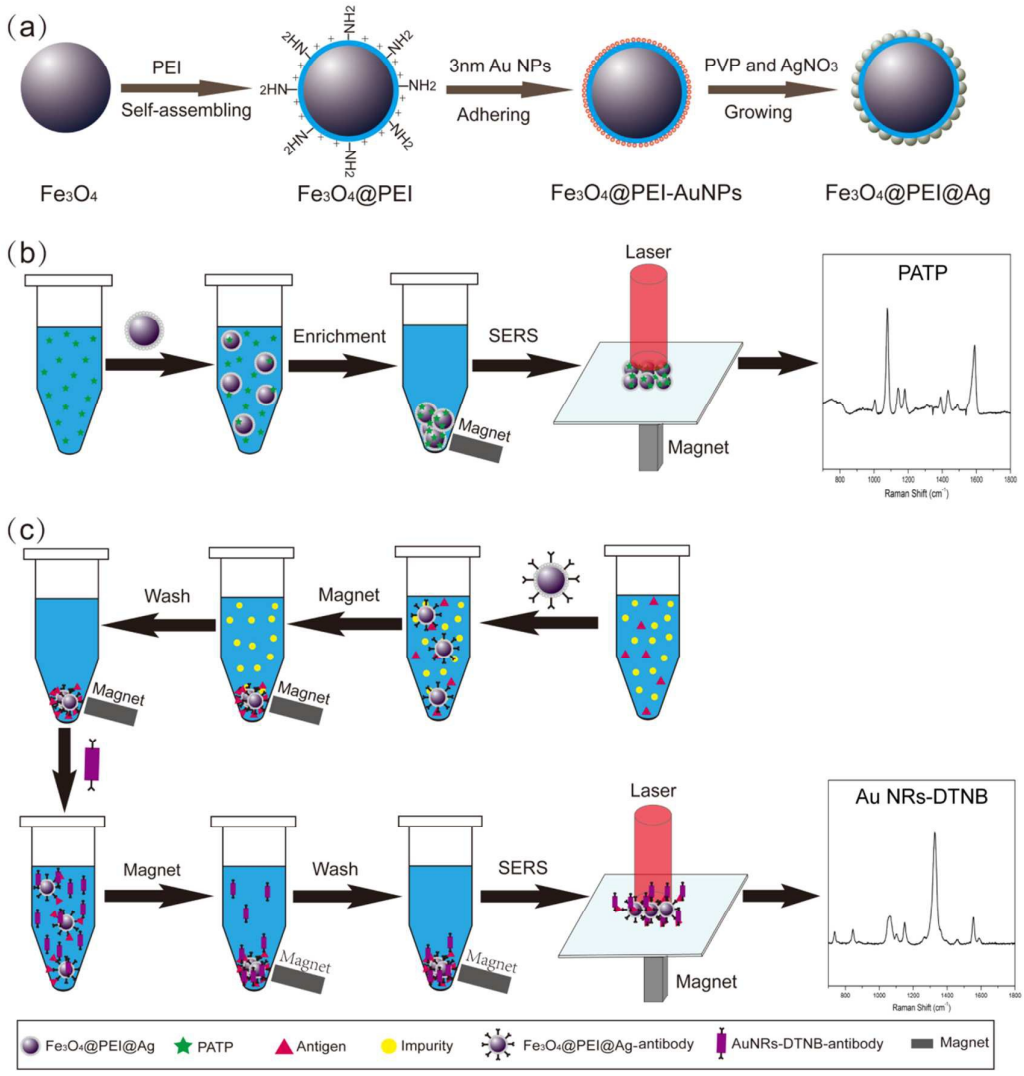

Scheme 1. (a) The synthesis procedure of Fe_3O_4@PEI@Ag microspheres. (b) The SERS detection protocol for specific binding molecule using Fe_3O_4@PEI@Ag microspheres as active substrates. (c) The aqueous phase immunoassay protocol for SERS-based sandwich assay using Fe_3O_4@PEI@Ag microspheres as active substrates.

Fabrication of the Fe_3O_4@PEI@Ag microspheres

As illustrated in Scheme 1(a), the Fe_3O_4@PEI@Ag microspheres were synthesized in four steps. Firstly, we synthesized 250 nm Fe_3O_4 nanoparticles through a typical solvothermal reaction at 210°C by reduction of $FeCl_3$ with ethylene glycol in the presence of NaAc as an alkali source and PEG6000 as a stabilizer. Secondly, the Fe_3O_4@PEI microspheres were prepared with the cationic PEI self-assembled on the surface of magnetic particles under sonication condition. PEI has plenty of primary amine groups and good hydrophilicity, which can significantly improve the dispersion of the magnetic particles.[24] Thirdly, many negatively charged 3 nm Au NPs were absorbed on the surface of Fe_3O_4@PEI as seeds by positive electricity of PEI. Moreover, the Au NPs were attached firmly to the Fe_3O_4 microspheres by sonicating due to the covalent binding between the -NH_2 groups of

the PEI and Au nanoparticles.[25, 26] Fourthly, Fe_3O_4@PEI@Ag core-shell microspheres were quickly obtained through a seed-mediated growth method. The isotropic growth of all the Au seed in a few seconds and the stabilization provided by PVP are essential for obtaining complete Ag shells.

Characterization of Fe_3O_4@PEI@Ag microspheres

The size and shape of the as-obtained products were characterized by transmission electron microscope (TEM) and scanning electron microscope (SEM). Fig. 1(a) shows a representative TEM image of the Fe_3O_4 microspheres. The prepared monodispersed Fe_3O_4 particles had a diameter of approximately 250 nm. Hydrophilic PEI self-assembled on the surface of Fe_3O_4 microspheres easily and can significantly improve the dispersity of particles (Fig. 1b). To confirm that the PEI had been successfully self-assembled on the Fe_3O_4 microspheres, we use high-resolution TEM (HRTEM) to monitor the thickness of the PEI shell. HRTEM images of Fig. 1(c) proved that PEI self-assembled on the Fe_3O_4 microspheres to form a thin shell under 60 min sonicating reaction, with thickness of around 2 nm. The PEI-coating progress was also confirmed by Zeta potential measurement, in which the ζ-potential increases obviously from −29.6 mV to +38.5 mV**,** hinting that positively charged PEI were completely assembled onto the surface of Fe_3O_4. Fig. 1(d) shows that dense small Au nanoparticles spreaded uniformly on the surface of the Fe_3O_4@PEI particles. Meanwhile, the absorption of Au NPs was also confirmed by the SEM image (Fig. 1f). Herein, we use a "seed-mediated growth" method to form complete and uniform Ag shell. Continuous and rough edges were seen around the Fe_3O_4@PEI@Ag microspheres, but we failed to observe the core-shell structure in one microsphere, because that Ag shell of the obtained microspheres can not be penetrated by the electron beam (Fig. 1e). As is evident from the SEM image shown in Fig. 1(g), many large size Ag-NPs covered the entire surface of the Fe_3O_4 microspheres, which formed a complete shell with nanoscale roughness.

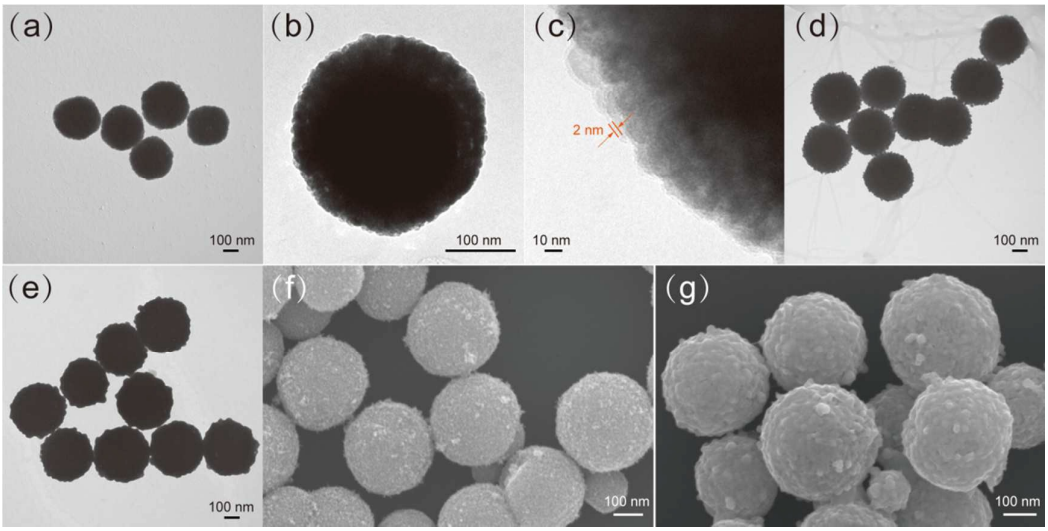

Figure 1. TEM images of (a) Fe_3O_4 microspheres, (b) Fe_3O_4@PEI, and (c) the corresponding magnified HRTEM image of its edge (arrows indicate a thin shell of PEI), (d) Fe_3O_4@PEI-Au seed, (e) Fe_3O_4@PEI@Ag microspheres, and SEM images of (f) Fe_3O_4@PEI-Au seed, (g) Fe_3O_4@PEI@Ag microspheres.

The strategy of Ag shell formation used here is a "seed-mediated growth" method. It is well known that the seed-mediated growth method is a universal approach to grow metal particles by adding new atoms onto the existing nuclei.[27] Few new nuclei form in the growth process due to the low concentration of reactant, which is beneficial for synthesis of particles with narrow size distribution.[28] Although the rapid reaction in the growth step

is rarely used in common seed-mediated reaction, it is important in our strategy, as the morphology of silver shells is determined by the kinetic factor. The 3 nm Au NPs on the Fe_3O_4 herein acts as nucleation sites for the deposition of Ag shell, therefore, the existence of uniform 3 nm Au NPs attached to the PEI-coated Fe_3O_4 microsphere is necessary in our experiment. When ammonia was added, Ag^+ was reduced by formaldehyde in a few seconds and deposited on the Au seeds of Fe_3O_4@PEI, resulting in complete Ag shells surrounding the Fe_3O_4 microspheres. It should be noted that PVP is used to avoid aggregation of core-shell microspheres and to control the growth of Ag shells.[27] PVP wholly covered all the facets of Au seeds, which facilitated isotropic growth of Ag particles, which played a key role in forming uniform Ag shells. As described in the experimental section, PVP concentration is kept at 0.2% wt, and the Fe_3O_4@PEI-Au seed microspheres are maintained at 10 mg in a 100 mL reaction system, while that of $AgNO_3$ amount is subjected to variation during all experiments. As shown in Fig. 2(a-f), with the increasing amount of $AgNO_3$ in the reaction system (0-4 mg), the Ag shell is changed from discontinuous to continuous. When the amount of $AgNO_3$ increased to 4 mg, the uniform and complete Ag shell of each microsphere with about 30 nm thickness is obtained. These experimental results indicate that the coverage and size of the Ag-NPs shell can be well controlled by increasing the amount of $AgNO_3$ from 0 to 4 mg while keeping all other parameters fixed.

Fig. 2(g) shows the UV-vis spectra of Fe_3O_4@PEI@Ag microspheres prepared with different amount of $AgNO_3$. Prior for the UV-vis spectra, the Fe3O4@PEI@Ag microspheres were washed and redispersed into water solution, and then subjected to gentle sonication. The UV-vis spectrum of Fe_3O_4 microspheres is shown as curve a- of Fig. 2g. A broad plasmon band observed for the Fe_3O_4 could be explained in terms of particles heterogeneity, from magnetic cores and tips polydispersity. The Fe_3O_4@PEI-Au seed microspheres did not show any obvious UV-visible absorption (curve b- of Fig. 2g). This phenomenon can be explained that PEI-coating significantly improved the dispersion of particles, while the 3nm Au seeds are too small to impact the microspheres' structure to induce plasmonic coupling. Upon the formation of the Ag shell, the absorbance appeared approximately 450 nm due to a Mie plasmon resonance excitation from the silver nanoparticles.[13] Evidently, the plasmon resonance peak became red-shifted gradually, while the surface plasmon absorption band of Ag deposited on the Fe_3O_4@PEI surface broadened as the amount of $AgNO_3$ increased (curve c-g of Fig 2.g). The change of the plasmon resonance peak aslo indicated that the Ag shell from discontinuous to continuous.

To characterize the sensitivity of these Fe_3O_4@PEI@Ag microspheres, the enhancement ability is estimated with the PATP as the model SERS probe. The PATP is a common Raman probe having the outstanding affinity to Au/Ag surfaces and a large Raman cross-section.[29-31] Fig. 2(h) showed the SERS spectra of PATP (10^{-7} M) adsorbed onto Fe_3O_4@PEI@Ag that have been prepared with different amount of $AgNO_3$, which were 0, 0.5, 1, 2, 3, and 4 mg, respectively. All the feature peaks at 1590, 1430, 1389, 1180, 1143 and 1077 cm^{-1} of PATP were observed and agreed well with the previously reported[29]. Futhermore, the intensity of the SERS peaks was increased with the high feeding amount of $AgNO_3$. Obviously, the Fe_3O_4@PEI-Au seed (0 mg $AgNO_3$) exhibited no enhancement effect (curve a of Fig. 2h) and the Fe_3O_4@PEI@Ag (0.5-4 mg $AgNO_3$) possessed the gradually increase enhancement with the increase of the Ag shell (curve b-f of Fig. 2h). The best-performing microspheres were Fe_3O_4@PEI@Ag (4 mg $AgNO_3$), which showed that the complete Ag shell had greater surface plasmon efficiency. However, when the amount of $AgNO_3$ increased to 5 mg, the intensity of the PATP SERS peaks became no further enhanced than that of the Fe_3O_4@PEI@Ag with 4 mg $AgNO_3$ (data not shown). The results suggest that the SERS activity of the Fe_3O_4@PEI@Ag microspheres arises mainly from the plasma effect due to the shell geometry of the Ag nanoparticles, and the continuous Ag shell has greater surface plasmon efficiency. Moreover, the uniform and complete Ag shell benefits the structural reproducibility and signal stability.

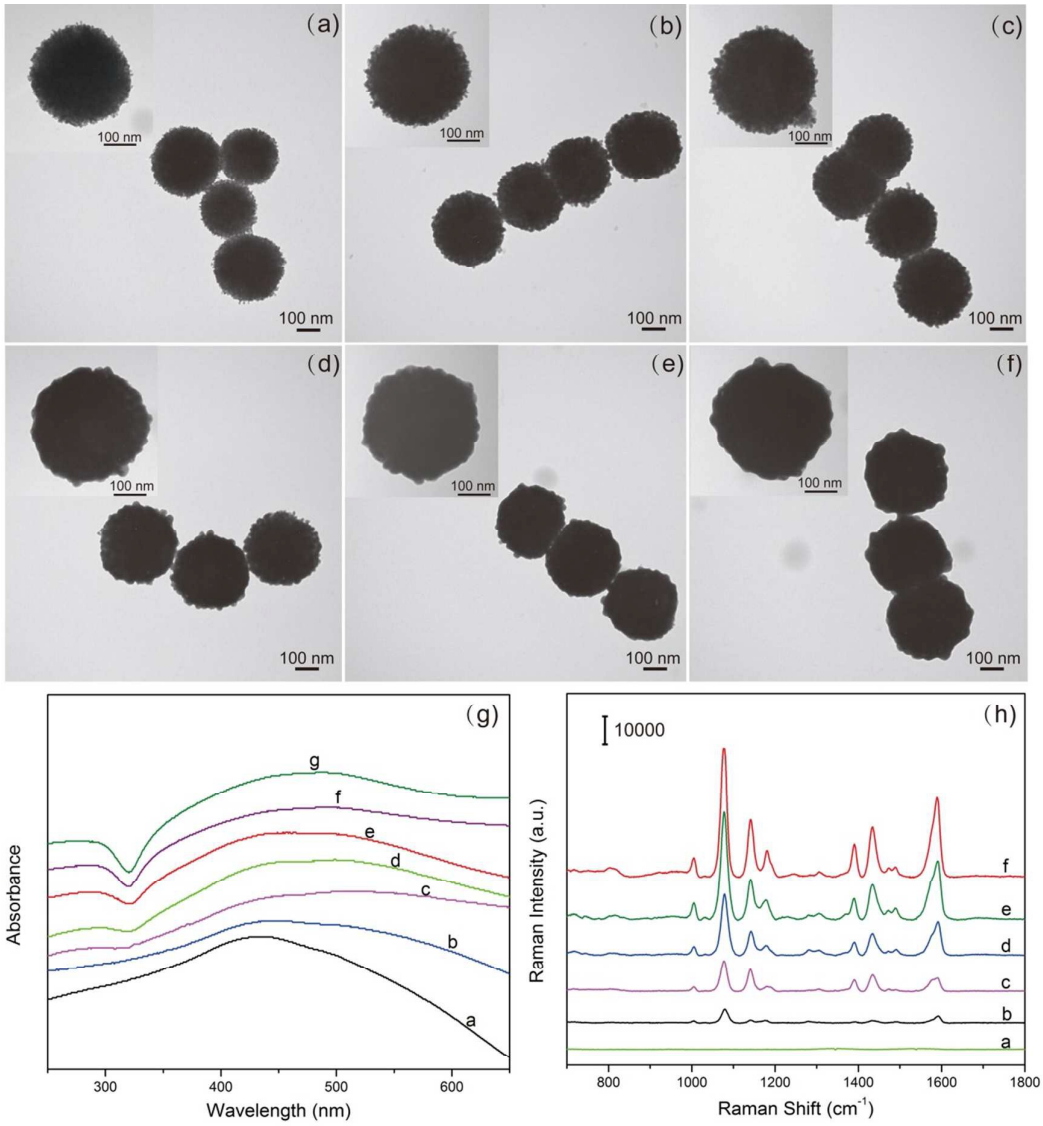

Figure 2. (a-f) TEM images of Fe_3O_4@PEI@Ag synthesized with different amount $AgNO_3$. (a) 0 mg, (b) 0.5 mg, (c) 1 mg, (d) 2 mg, (e) 3 mg, (d) 4 mg. Insets (a-f) are enlarged images of a single particle. (g) UV-visible spectra of a- Fe_3O_4, b- Fe_3O_4@PEI-Au seed, and c-g- Fe_3O_4@PEI@Ag parepared with following amount $AgNO_3$: c-0.5 mg, d- 1 mg, e- 2 mg, f- 3 mg, g- 4 mg. (h) Raman spectra of PATP (10^{-7} M) using Fe_3O_4@PEI@Ag microspheres prepared with different amount $AgNO_3$. a- 0 mg, b- 0.5 mg, c- 1 mg, d- 2 mg, e- 3 mg, f- 4 mg.

Powder X-ray diffraction (XRD) has been used to confirm the crystal structure and phase purity of main synthetic product (Fig. 3a). Curve a- in Fig. 3(a) showed the typical XRD pattern of the Fe_3O_4 nanoparticles. The diffraction peaks at 2θ values of 30°, 37.1°, 43°, 56.9°, and 62.5° refer to (112), (202), (220), (303), and (224) planes of cubic inverse spinel Fe_3O_4, respectively, which could all be indexed to the cubic structure of Fe_3O_4 (JCPDS No.75-1609).[32] After the absorption of 3 nm Au NPs on the Fe_3O_4, a new XRD peak was observed at a 2θ value of 38.2°, which corresponded to the (111) crystal planes of cubic phase Au (JCPDS No.04-0784), as shown in curve b- of Fig. 3(a).[33] No diffraction peaks corresponding to PEI are observed because the PEI layer is amorphous. Curve c- of Fig 3(a) showed a typical XRD pattern of the Fe_3O_4@PEI@Ag sample. In addition to the

diffraction peaks that corresponded to Fe_3O_4, there existed four other strong diffraction peaks refer to (111), (200), (220) and (311) crystalline planes of cubic Ag (JCPDS card No. 04-0783), respectively.[34]

The magnetic properties of the resulting products were investigated using a superconducting quantum interference device magnetometer (SQUID, MPMSXL-7) at 300K. As shown in Figure 3(b), the saturation magnetization (MS) of the Fe_3O_4, Fe_3O_4@PEI-Au seed, and Fe_3O_4@PEI@Ag were found to be 76.5, 65.1, and 54.3 emu/g, respectively. The MS values tended to decrease slightly after the process of PEI-coating, Au seed-absorbing and Ag shell-forming. The lower Ms of the Fe_3O_4@PEI-Au seed and Fe_3O_4@PEI@Ag microspheres compared with the Fe_3O_4 particles can be explained by nonmagnetic coating materials surrounding the Fe_3O_4 cores. All of the curves nearly intersect with the origin, which shows that all of the three products were in a superparamagnetic state at room temperature.[15] In the practical magnetic separation test, the Fe_3O_4@PEI@Ag could be completely separated from the solution within only 10 s when the magnetic field was applied (the inset image of Fig. 3b). Such a short separation time reflected the potential of the Fe_3O_4@PEI@Ag microspheres for the rapid enrichment of target analyte.

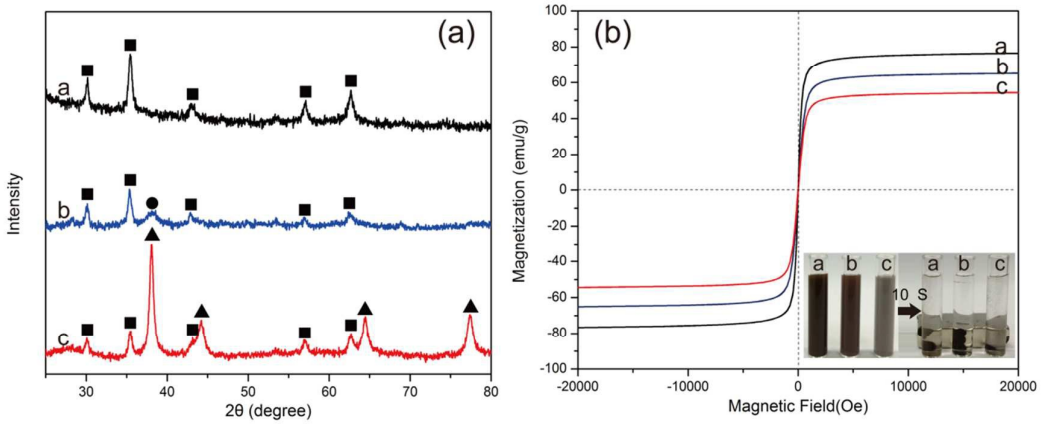

Figure 3. Typical XRD patterns (a) and magnetic hysteresis curves (b) of a- Fe_3O_4, b- Fe3O_4@PEI-Au seed and c-Fe_3O_4@PEI@Ag microspheres. Inset: Magnetic separation behaviors of above three products in the solution. The squares label the peaks of the magnetite structure of Fe_3O_4, the circles label the peaks of cubic Au and the triangles label the peaks of cubic Ag.

It is worth mentioning that we first proposed the PEI-assisted "seed-mediated growth" method is widely used in the synthesis of various Ag-coated magnetic core-shell microspheres ranging from 100 nm to 800 nm. Fig. 4(a-d) show TEM images of single Fe_3O_4@PEI-Au seed microsphere with different sizes (200-500 nm), and Fig. 4(e-f) clearly show their corresponding fabricated Fe_3O_4@PEI@Ag microspheres, respectively. Ag-coated magnetic microspheres with different size can be used for different purposes. In this study, we chose 250 nm Fe_3O_4 microspheres as the core to fabricate Fe_3O_4@PEI@Ag with 0.4 mg $AgNO_3$. The as-obtained products possess good dispersity, strong magnetic responsiveness, and excellent SERS ability at the same time, and are very suitable for SERS based immunoassay in the solution.

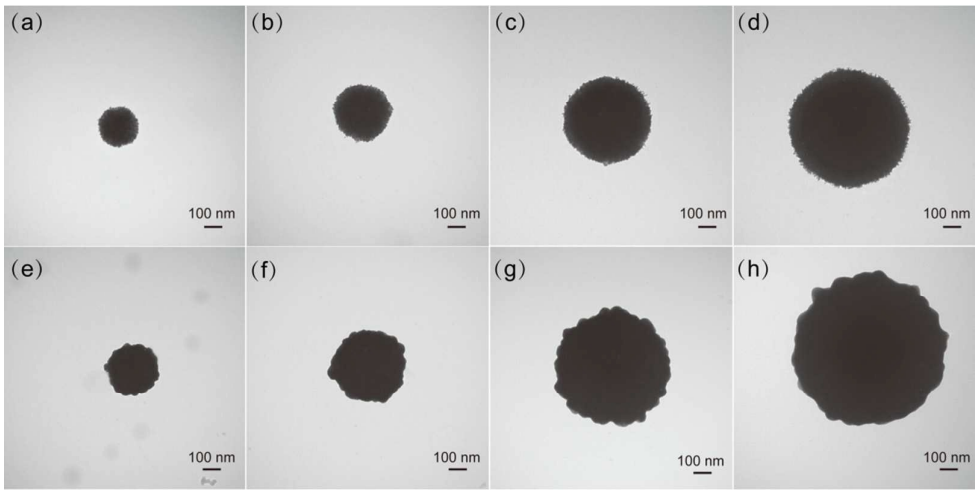

Figure 4. (a-d) TEM images of Fe_3O_4@PEI-Au seed with different sizes: (a) 200 nm, (b) 300 nm, (c) 400 nm, (d) 500 nm, and their corresponding fabricated Fe_3O_4@PEI@Ag microspheres (e), (f), (g), (h), respectively.

The SERS activity of Fe_3O_4@PEI@Ag microspheres

For the determination of the SERS sensitivity of the 300nm-scale Fe_3O_4@PEI@Ag, a series of PATP alcoholic solutions with variable concentration ranging from 10^{-6} to 10^{-12} M were prepared accurately. The detail operation process was introduced in Experiment section, as illustrated in Scheme 1(b). The SERS spectra were recorded as shown in Fig. 5(a). All major vibrational modes of PATP can be clearly shown at the concentration of 10^{-11} M. Fig. 5(b) shows the plot of the intensity measured at 1077 cm^{-1} as a function of PATP concentration. The error bars indicated the standard deviations from 5 measurements. The dose-response SERS spectra of serial dilutions of samples facilitate the quantitative detection of the adsorbed molecules with Fe_3O_4@PEI@Ag microspheres as an active SERS substrate.

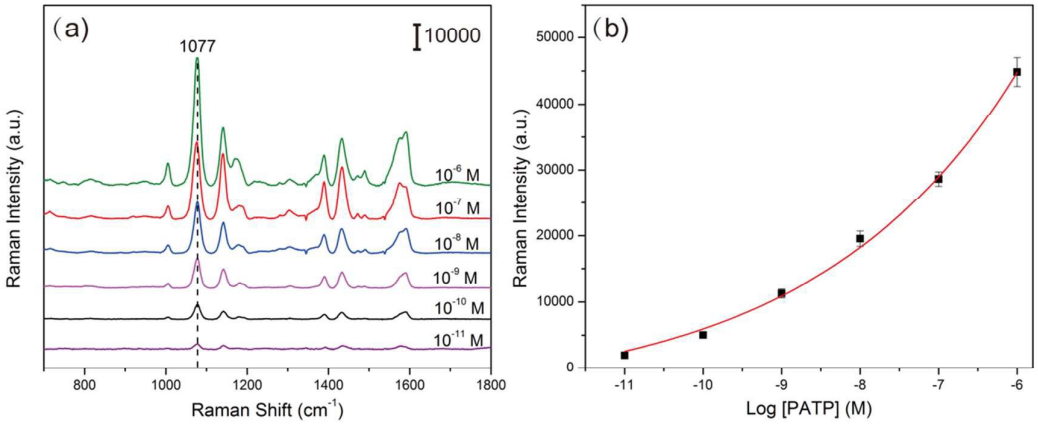

Figure 5. (a) The SERS spectra of PATP measured with different concentrations on the Fe_3O_4@PEI@Ag microspheres. (b) Calibration curve for PATP detection (R^2 = 0.995). The error bars represent the standard deviations from 5 measurements.

The Fe_3O_4@PEI@Ag based SERS immunoassay for detecting human IgG detection

The synthesized Au NRs were characterized by TEM image with dimensions of approximately 75 nm × 18 nm (Fig. 6a). Au NRs with a few irregular large particles were successfully synthesized by adding a proper amount of

HCl. These Au NRs were modified with 10 μM DTNB under sonication for 1 h. Fig. 6(b) shows the extinction spectra of Au NRs (black curve) and Au NRs-DTNB (red curve). The Au NRs show a longitudinal SPR (LSPR) peak at around 800 nm and a transverse SPR (TSPR) peak at 511 nm, indicating a rod shape of the Au NRs.[35] Moreover, the figure shows that DTNB exerted no influence on the LSPR wavelength of Au NRs. In order to confirm the SERS activity of Au NRs, the same concentration of SERS reporters should be added to an equal volume of the nanorods solution. Fig. 6(c) shows the Raman spectra of the synthesized Au NRs-DTNB, the signal of the Au NRs-DTNB is strong enough for the subsequent SERS immunoassay.

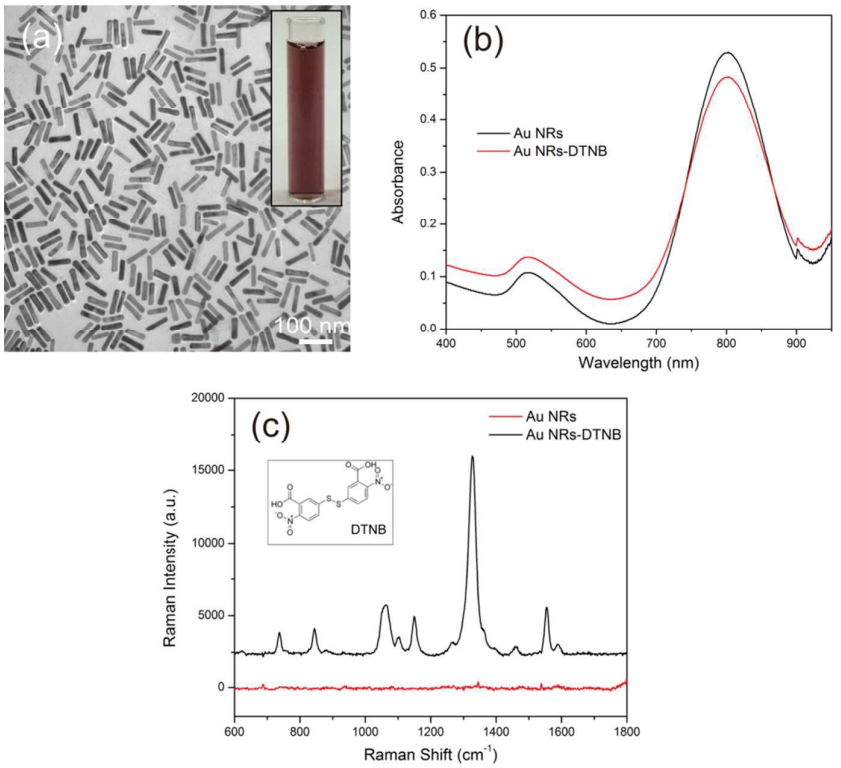

Figure 6. Characterization of the property of Au NRs-DTNB as SERS-tags. (a) TEM images of Au NRs. (b) UV-visible spectra of Au NRs and Au NRs-DTNB. (c) Raman intensity of Au NRs-DTNB was measured at the 785 nm excitation.

Scheme 1(c) represents the operating principle of the Fe_3O_4@PEI@Ag (300 nm-scale) based SERS immunoassay, and human IgG is selected as the model target biomolecules to explore the sensitivity of the presented immunoassay protocol. Our designed SERS immunoassay is based on sandwich-type configuration of antibody/antigen/antibody interaction.[36] In the experiments, different concentration of human IgG were added to 8 groups of solutions containing goat anti-human IgG modified Fe_3O_4@PEI@Ag microspheres and mouse anti-human IgG modified Au NRs-DTNB, resulting in final concentrations of human IgG ranging from 10^{-6} g/ml to 10^{-14} g/mL. For the blank control, 1 % BSA was added instead of the human IgG. Incubated at room temperature for 1 h, each group of the mixture solution was enriched by a magnet. After washing with PBST under magnetic confinement to remove the free SERS tags, the resultant immune-Au NRs-DTNB/human IgG/immune-Fe_3O_4@PEI@Ag precipitates was resuspended in water and dropped on a silicon substrate. After drying in air, SERS spectroscopy and imaging were conducted.

Fig. 7(a) shows the human IgG concentration-dependent SERS spectra of Au NRs-DTNB based immunoassay. The spectra were obtained by averaging five readings at the point of each sample in the range of 10^{-6} g/ml to 10^{-14}

g/ml. By using symmetric NO_2 stretching bands of DTNB (peak intensity at 1328 cm^{-1}) to characterize SERS detection, we plotted the dose-response calibration curve shown in Fig. 7(b). Since the limit of detection (LOD) is defined as the analyte concentration that produces a signal three times larger than the standard deviation of the blank control, the LOD of the immunoassay protocol was 10^{-14} g/mL (10 fg/mL). From above results, we have demonstrated the great potential of these Fe_3O_4@PEI@Ag microspheres for highly selective and sensitive protein detection with the help of SERS tags.

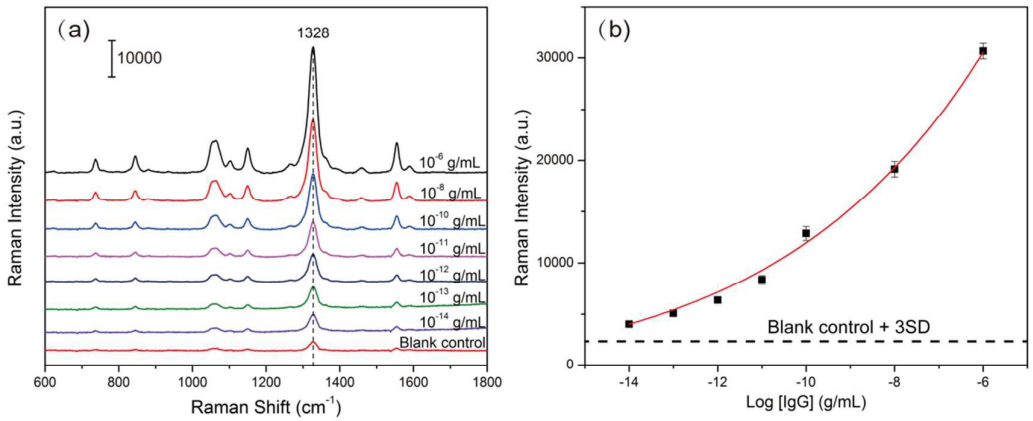

Figure 7. (a) SERS spectra of the sandwich complex at different human IgG concentrations. (b) Dose-response curve of the above SERS-based immunoassay (R^2 = 0.992). The error bars represent the standard deviations from 5 measurements.

CONCLUSIONS

In summary, we reported a facile and effective method for fabrication of novel PEI-interlayered silver-shell magnetic-core microspheres with monodispersity, high magnetization property and complete Ag shell, in which PEI are skillfully used to absorb 3 nm Au NPs as seed and prevent particle aggregation. The size and coverage level of the Ag-NPs shell on Fe_3O_4@PEI@Ag microspheres were shown to be easily controlled by varying the amount of $AgNO_3$. Moreover, this method is a universal route for Ag shell deposition onto magnetic microspheres ranging from 100 to 800 nm. The detailed nanostructures of the Fe_3O_4@PEI@Ag microspheres were characterized by TEM, SEM, XRD, and UV-visible spectroscopy. In addition, the micro-scale Fe_3O_4@PEI@Ag can be separated from the sample solution rapidly, which shortens the detection time and enriches the target analytes. The SERS ability test results show that PATP in the solution with a concentration as low as 10^{-11} M could be detected. Meanwhile, the Fe_3O_4@PEI@Ag based SERS immunoassay results show that human IgG in the mixed solution could be quantitative detection as low as 10 fg/mL, with the help of SERS tags. Therefore, this kind of Fe_3O_4@PEI@Ag microsphere would be very useful as a multifunctional SERS substrate for detecting molecule analytes and target protein in the solution.

Acknowledgements

This work was supported by the National Natural Science Foundation of China under Grant No.51475468 and Chinese National Instrumentation Program No. 2012YQ18017

Notes and references

[a]College of Life Sciences & Bio-Engineering, Beijing University of Technology, Beijing 100124. E-mail: sqwang@bmi.ac.cn.

[b]Beijing Institute of Radiation Medicine, Academy of Military Medical Sciences, Beijing 100850, PR China. E-mail: ruixiao203@sina.com.

[c] College of Optoelectronic Science and Engineering, National University of Defense Technology, Changsha 410073, China.

[d]College of Mechatronics and Automation, National University of Defense Technology, Changsha, Hunan 410073, PR China.

‡ These authors contributed equally to this work.

1. J. F. Li, Y. F. Huang, Y. Ding, Z. L. Yang, S. B. Li, X. S. Zhou, F. R. Fan, W. Zhang, Z. Y. Zhou, Y. Wu de, B. Ren, Z. L. Wang and Z. Q. Tian, *Nature*, 2010, **464**, 392-395.
2. S. Y. Lee, S.-H. Kim, M. P. Kim, H. C. Jeon, H. Kang, H. J. Kim, B. J. Kim and S.-M. Yang, *Chemistry of Materials*, 2013, **25**, 2421-2426.
3. Y. Zhou, X. Cheng, D. Du, J. Yang, N. Zhao, S. Ma, T. Zhong and Y. Lin, *Journal of Materials Chemistry C*, 2014, **2**, 6850.
4. J. F. Li, X. D. Tian, S. B. Li, J. R. Anema, Z. L. Yang, Y. Ding, Y. F. Wu, Y. M. Zeng, Q. Z. Chen, B. Ren, Z. L. Wang and Z. Q. Tian, *Nature protocols*, 2013, **8**, 52-65.
5. C. Wang, R. Xiao, X. Wu, P. Dong, Z. Rong, J. Chen and S. Wang, *Laser Physics*, 2014, **24**, 045807.
6. A. K. Samal, L. Polavarapu, S. Rodal-Cedeira, L. M. Liz-Marzán, J. Pérez-Juste and I. Pastoriza-Santos, *Langmuir : the ACS journal of surfaces and colloids*, 2013, **29**, 15076-15082.
7. J. F. Wang, X. Z. Wu, R. Xiao, P. T. Dong and C. G. Wang, *PLoS ONE*, 2014, **9**, e97976.
8. J. Liu, S. Z. Qiao, Q. H. Hu and G. Q. Lu, *Small*, 2011, **7**, 425-443.
9. J. M. Li, W. F. Ma, L. J. You, J. Guo, J. Hu and C. C. Wang, *Langmuir : the ACS journal of surfaces and colloids*, 2013, **29**, 6147-6155.
10. W.-F. Ma, Y. Zhang, L.-L. Li, L.-J. You, P. Zhang, Y.-T. Zhang, J.-M. Li, M. Yu, J. Guo, H.-J. Lu and C.-C. Wang, *ACS Nano*, 2012, **6**, 3179-3188.
11. H. Guo, A. Zhao, Q. Gao, D. Li, M. Zhang, Z. Gan, D. Wang, W. Tao and X. Chen, *Journal of Nanoparticle Research*, 2014, **16**.
12. X. X. Han, A. M. Schmidt, G. Marten, A. Fischer, I. M. Weidinger and P. Hildebrandt, *ACS Nano*, 2013, **7**, 3212-3220.
13. Q. An, P. Zhang, J. M. Li, W. F. Ma, J. Guo, J. Hu and C. C. Wang, *Nanoscale*, 2012, **4**, 5210-5216.
14. J. Shen, Y. Zhu, X. Yang, J. Zong and C. Li, *Langmuir : the ACS journal of surfaces and colloids*, 2013, **29**, 690-695.
15. Y. Wang, K. Wang, B. Zou, T. Gao, X. Zhang, Z. Du and S. Zhou, *Journal of Materials Chemistry C*, 2013, **1**, 2441.
16. H. Hu, Z. Wang, L. Pan, S. Zhao and S. Zhu, *The Journal of Physical Chemistry C*, 2010, **114**, 7738-7742.
17. M. Zhu, C. Wang, D. Meng and G. Diao, *Journal of Materials Chemistry A*, 2013, **1**, 2118.
18. H. Deng, X. Li, Q. Peng, X. Wang, J. Chen and Y. Li, *Angewandte Chemie*, 2005, **117**, 2842-2845.

19. Y. Fang, S. Guo, C. Zhu, Y. Zhai and E. Wang, *Langmuir : the ACS journal of surfaces and colloids*, 2010, **26**, 11277-11282.
20. B. Nikoobakht and M. A. El-Sayed, *Chemistry of Materials*, 2003, **15**, 1957-1962.
21. B. Zhao, J. Shen, S. Chen, D. Wang, F. Li, S. Mathur, S. Song and C. Fan, *Chem. Sci.*, 2014, **5**, 4460-4466.
22. Z. Wang, S. Zong, W. Li, C. Wang, S. Xu, H. Chen and Y. Cui, *Journal of the American Chemical Society*, 2012, **134**, 2993-3000.
23. X. Qian, X. H. Peng, D. O. Ansari, Q. Yin-Goen, G. Z. Chen, D. M. Shin, L. Yang, A. N. Young, M. D. Wang and S. Nie, *Nature biotechnology*, 2008, **26**, 83-90.
24. L. Lou, K. Yu, Z. Zhang, B. Li, J. Zhu, Y. Wang, R. Huang and Z. Zhu, *Nanoscale*, 2011, **3**, 2315.
25. L. Lou, K. Yu, Z. Zhang, R. Huang, J. Zhu, Y. Wang and Z. Zhu, *Nano Research*, 2012, **5**, 272-282.
26. L. Lou, K. Yu, Z. Zhang, R. Huang, Y. Wang and Z. Zhu, *Applied Surface Science*, 2012, **258**, 8521-8526.
27. T. Liu, D. Li, D. Yang and M. Jiang, *Colloids and Surfaces A: Physicochemical and Engineering Aspects*, 2011, **387**, 17-22.
28. S. Zhang, F. Ren, W. Wu, J. Zhou, L. Sun, X. Xiao and C. Jiang, *Journal of Nanoparticle Research*, 2012, **14**.
29. J.-M. Li, W.-F. Ma, C. Wei, J. Guo, J. Hu and C.-C. Wang, *Journal of Materials Chemistry*, 2011, **21**, 5992.
30. K. Kim, D. Shin, H. B. Lee and K. S. Shin, *Chemical communications*, 2011, **47**, 2020-2022.
31. Y. F. Huang, D. Y. Wu, H. P. Zhu, L. B. Zhao, G. K. Liu, B. Ren and Z. Q. Tian, *Physical chemistry chemical physics : PCCP*, 2012, DOI: 10.1039/c2cp40558j.
32. Q. An, M. Yu, Y. Zhang, W. Ma, J. Guo and C. Wang, *The Journal of Physical Chemistry C*, 2012, **116**, 22432-22440.
33. U. Tamer, İ. H. Boyacı, E. Temur, A. Zengin, İ. Dincer and Y. Elerman, *Journal of Nanoparticle Research*, 2011, **13**, 3167-3176.
34. C. Li, J. Mei, S. Li, N. Lu, L. Wang, B. Chen and W. Dong, *Nanotechnology*, 2010, **21**, 245602.
35. X. Ye, L. Jin, H. Caglayan, J. Chen, G. Xing, C. Zheng, V. Doan-Nguyen, Y. Kang, N. Engheta, C. R. Kagan and C. B. Murray, *ACS Nano*, 2012, **6**, 2804-2817.
36. C. Song, Z. Wang, R. Zhang, J. Yang, X. Tan and Y. Cui, *Biosensors and Bioelectronics*, 2009, **25**, 826-831.
37. D. Graham and R. Goodacre, *Chemical Society reviews*, 2008, **37**, 883-884.

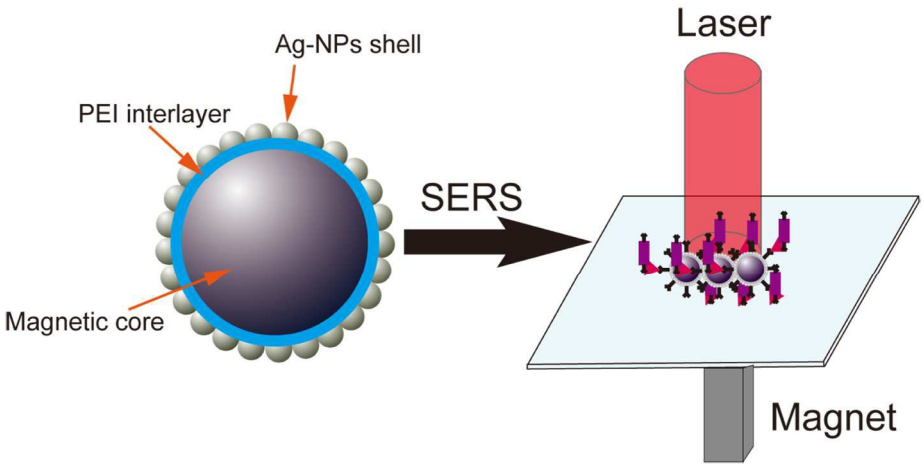

161x77mm (300 x 300 DPI)